



Factors that trigger the development of mining-induced ground fissures, and standards to treat them in shallow coal mining areas

H. Liu^{1,2}, T-T. Zhou¹, X. Liu¹, K-Z. Deng², and S-G. Lei²

Affiliation:

¹Anhui Province Engineering Laboratory for Mine Ecological Remediation, School of Resources and Environmental Engineering, Anhui University, China.

²State Key Laboratory of Coal Resource and Safe Mining, School of Environment Science and Spatial Informatics, China University of Mining and Technology, Xuzhou, China.

Correspondence to:

H. Liu

Email:

lhui99@aliyun.com; cumtdkz@sina.com; 12303183@qq.com

Dates:

Received: 30 Oct. 2018

Revised: 3 Jul. 2019

Accepted: 14 Jun. 2019

Published: November 2019

How to cite:

Liu, H., Zhou, T-T., Liu, X., Deng, K-Z., and Lei, S-G.

Factors that trigger the development of mining-induced ground fissures, and standards to treat them in shallow coal mining areas.

The Southern African Institute of Mining and Metallurgy

DOI ID:

<http://dx.doi.org/10.17159/2411-9717/415/2019>

ORCID ID:

H. Liu
<https://orcid.org/0000-0003-1949-7072>

Synopsis

The exploitation of shallow coal seams causes severe surface subsidence and triggers the development of numerous ground fissures, which threaten the safety of underground mining and damage the surface eco-environment. We studied the law of surface movement and the development of ground fissures at three panels in the Daliuta coal mine, Shendong mining district of western China. The results showed that mining-induced ground fissures developed in a cycle of 'crack-expand-close', and formed permanent cracks that were arranged in an elliptical shape on the edge of the goaf. There was a positive linear relationship between the fissure width and the surface horizontal deformation, as one would expect, and a positive logarithmic relationship between the fissure angle and the mining rate during coal face advancing. We propose a basis and standard for treating dynamic fissures which recommends that, to ensure the safety of underground mining, the fissures should be treated when the surface cracks extend as far as the fractured zone of rock strata. The results will support predictions of the development of mining-induced ground fissures so that disasters can be prevented in shallow coal seam mining areas.

Keywords

ground fissure, shallow coal seam, surface subsidence, angle of ground fissure, eco-environment protection.

Introduction and background

Coal mines in western China are generally shallow (less than 150 m), with thin rock strata (no more than 50 m) and thick, unconsolidated sand layers overlying the coal seams. It is widely accepted that the large-scale exploitation of coal resources results in considerable damage to the Earth's eco-environment (Bian *et al.*, 2012; Tost *et al.*, 2018). Mining-induced ground fissures develop frequently because of discontinuous deformation of the surface (Zhang, Lu, and Kim, 2018), which cause extensive damage to surrounding ecosystems and constitute a safety hazard during underground mining (Mohseni *et al.*, 2017), resulting in seepage and loss of surface and soil waters (He *et al.*, 2017; Li, Lei, and Shen, 2016). Vegetation withers and dies when soil moisture is lost through these ground fissures, such that the surrounding ecosystems are changed irreversibly (Dagvadorj, Byamba, and Ishikawa, 2018). Ground fissures also compromise the safety of underground mining activities, especially when these fissures extend downwards and connect with the fracture zone of strata, resulting in gas leakages, outbursts of water and sand, and other accidents (Hu, Wand, and He, 2014; Malinowska and Hejmanowski, 2016).

The Shendong mining area, where there are 14 world-class coal mines and coal reserves amounting to 223 Gt in total, is a good example of a concentrated large-scale coal mining area in an ecologically sensitive area of western China. The coal seams are thick, at shallow depths, and are generally overlain by a surface layer of thick loess and aeolian sands, and three to five layers of medium and fine sandstones.

This intensively-exploited area lacks water resources. The conflict between modern coal mining and the ecological fragility is the key constraint on the ongoing exploitation of the coal mines. When the overlying strata fracture and the surface subsides in the mining area, numerous ground fissures develop. For example, sand influx accidents have occurred frequently at panel 22402 of the Halagou coal mine. In one incident, aeolian sands flowed into the panel through rock fissures, such that a permanent funnel-shaped collapse pit 47 m in diameter and 12 m deep formed on the ground surface. As a consequence, production had to be stopped. Therefore, the issue of how to prevent and control ground fissure disasters is a major technical challenge for most coal mines, and studies of the development of mining-induced ground fissures are urgently needed.

Factors that trigger the development of mining-induced ground fissures



(a) Dynamic ground fissure



(b) Permanent ground fissure

Figure 1—Mining-induced ground fissures

Surface deformation in a mining area generally evolves over time. Damage to the rock strata, surface damage, and ground fissures also evolve over time as mining advances. Depending on when they develop, ground fissures may be divided into two types (Liu *et al.*, 2013): dynamic ground fissures that develop during mining and permanent ground fissures that develop after surface subsidence. Dynamic ground fissures usually develop above the panel when the strata rupture and the surface cracks; these fissures tend to develop rapidly and are self-healing, as shown in Figure 1a. Dynamic ground fissures threaten the safety of underground mining, especially when the cracks extend to the fractured zone of the rock strata, where sand outbursts and gas leakages may occur. Permanent ground fissures, which are generally wide, deep, and non-healable, usually develop on the surface above the boundary of the goaf, where the most stretching and deformation occurs. Large numbers of ground fissures close together cause surface fractures, soil erosion, and vegetation degradation, with consequences for the already fragile eco-environment, as shown in Figure 1b.

To date, researchers have used various approaches to examine the characteristics of ground fissures that have developed in different underground coal mining settings, including field measurements (Sun *et al.*, 2015; Finfinger and Peng, 2016), physical and computer numerical simulations (Ghabraie, Ren, and Smith, 2017; Yang *et al.*, 2018), and remote sensing images (Zhang, Lu, and Kim, 2018; Zhao *et al.*, 2019). These studies found that dynamic ground fissures often developed ahead of the advance of the panel (Gaur, Kar, and Srivastava, 2015). Although dynamic ground fissures can self-heal as mining advances, they pose a significant threat to the safety of underground operations (Salmi, Nazem, and Karakus 2017a). Ground fissures, however, do not always self-heal; several ground fissures distributed in the surface tensile zone on the margin of a panel did not self-heal when the ground subsided and so compromised the integrity of the surface eco-environment (Peng *et al.*, 2016). Other researchers studied the main influences on the development of mining-induced ground fissures, and examined the relationships between ground fissures and the mining conditions, such as the mining depth (Song *et al.*, 2016), thickness of the coal bed (Salmi, Nazem, and Karakus, 2017b), surface topography (Liu *et al.*, 2015; Yin and Dong, 2015; Ishwar and Kumar, 2017), and the soil characteristics (Han *et al.*, 2014; Wang, Li, and Wang, 2017), and found that the depth of the coal seam, the extraction height, and the thin unconsolidated surface layers were the main factors that influenced the development of ground fissures (Yang *et al.*, 2016; Zhao *et al.*, 2016). Some scholars explored the mechanisms that controlled the development of mining-induced ground fissures

in the context of various theories, including rock failure theory, surface deformation theory, and slope slip mechanisms. They established a mechanical model that described the formation of mining-induced ground fissures, and found that fractures in rocks and soil caused by underground mining were fundamental to the formation of ground fissures (Hartlieb *et al.*, 2017; Zhu *et al.*, 2019).

The abovementioned studies provide useful information about the development of mining-induced ground fissures. However, the effects of local mining conditions on the development of ground fissures need to be studied further. First, because of the constraints imposed by field conditions, it is difficult to obtain accurate information about how ground fissures evolve during mining, and there is also uncertainty about what technical methods should be used to obtain sufficient field data to describe the mechanisms that control the development of ground fissures. Secondly, although studies have shown that there is a linear relationship between the width of the ground fissure during development and the horizontal deformation of the surface, the factors that control the formation of the ground fissure are still not clear. Third, because dynamic fissures can self-heal (Malinowska and Hejmanowski, 2016), researchers have proposed that fissures should be remediated once the surface has stabilized after subsidence. However, engineers have found that the depth to which ground fissures and rock fractures penetrate influences the safety of the mining operations, especially in shallow coal mines. What mechanisms therefore influence the depth to which ground fissures penetrate? Under what conditions can ground fissures connect with the water-flowing fractured zone? At present, there are no clear guidelines for managing dynamic fissures. The overall aim of this study, therefore, was to gain further insights into how mining influenced the formation of ground fissures, using the shallow coal seam of the Shendong coal mining area as the study site. Specifically, we observed mining-induced ground fissures *in situ*, and analysed the characteristics of surface deformation and the formation and development of ground fissures. We examined the relationships between the geological setting and mining conditions and the development of ground fissures, and proposed and tested a method for treating dynamic ground fissures. We hope that the findings from our study will provide the theoretical and technical basis for predicting and preventing the risks of ground-fissure disasters related to mining shallow coal seams.

Geological and mining conditions of the study region

The Shendong mining area is one of the seven largest coalfields in the world. Situated between 109°58'–110°30' E and 38°52'–39°38' N, it includes the southeastern part of the Ordos Plateau,

Factors that trigger the development of mining-induced ground fissures

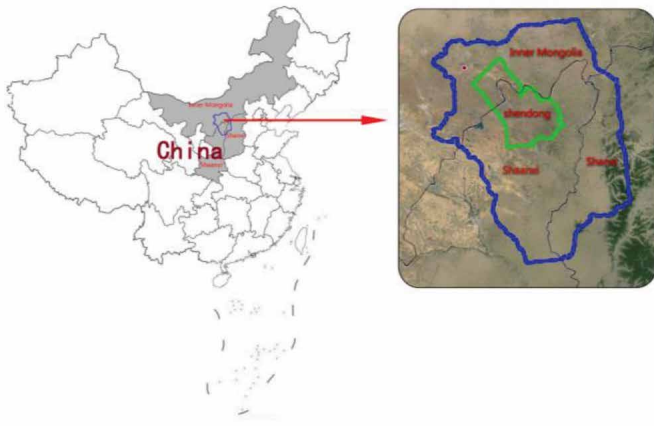


Figure 2—Geographical map and geomorphology of Shendong mining area

the northern margin of the Loess Plateau in northern Shaanxi, the southeastern margin of the Mu Us Desert, and the border areas of Shanxi Province, Shaanxi Province, and the Autonomous Region of Inner Mongolia in China; more specifically, it includes the northern part of Shenmu County and the eastern part of Fugu County in Shaanxi Province, the southern part of Ejina Horo Banner, Dongsheng City, and the southwestern part of

Jungar Banner in the Autonomous Region of Inner Mongolia. The mining area, shown in Figure 2, has an average elevation of 1200 m and extends over approximately 3 500 km².

Tectonically, the Shendong mining area belongs to the Ordos Basin. It has a simple structure, and does not contain large or medium-sized faults or well-developed rock fractures. It is overlain mainly by medium or hard rocks, such as fine sandstones, siltstones, and medium sandstones. The surface is covered with Quaternary loess and aeolian sands and the soils are dominated by sandy soil, loessal soil, red soil, and silty soil that are, for the most part, poor quality, loosely structured, and poorly permeable (Wang, Li, and Wang, 2017).

The Daliuta coal mine exploits three main coal seams, known as the no. 1-2 seam, no. 2-2 seam, and no. 5-2 seam, all of which are near-horizontal and are inclined at angles of between 1° and 3°. In this study, we studied the three different deep panels. Supercritical mining was used on the three panels, and the surfaces were fully subsided. The mining was fully mechanized and the longwall mining along the strike caused serious ground subsidence and a large number of ground fissures. Mining conditions for the three panels are shown in Table 1, and the generalized stratigraphic columns are shown in Figure 3.

Table 1

Main technical parameters for the three panels

Panel (m)	Length (m)	Width (m)	Extraction height (m)	Mining depth (m)	Thickness of strata (m)	Thickness of unconsolidated layer (m)
12208	1537	155	7.3	40.4	33.2	7.2
22201	643	350	3.9	73.0	60.7	12.3
52304	4548	300	6.9	234.9	204.7	30.2

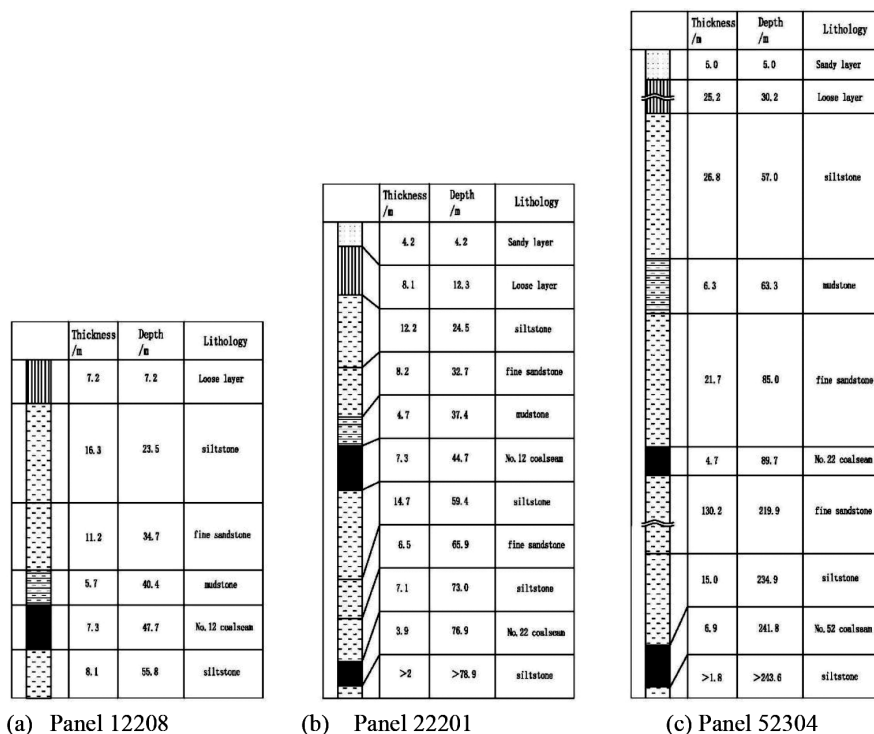


Figure 3—Stratigraphic columns of the three panels

Factors that trigger the development of mining-induced ground fissures

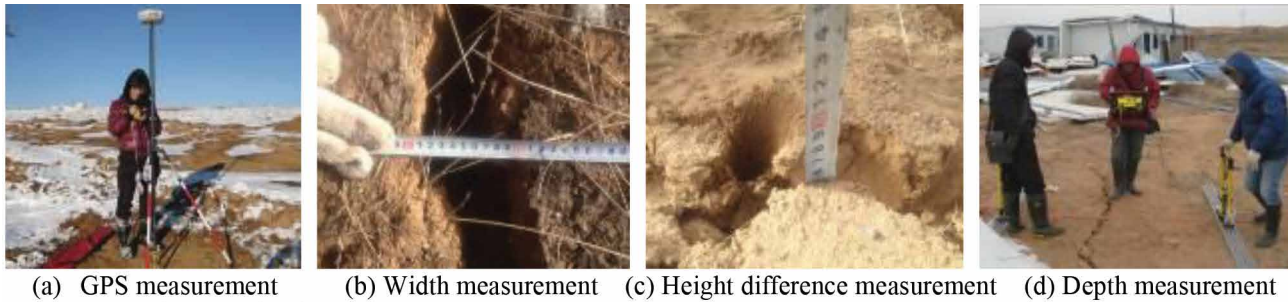


Figure 4—Field monitoring

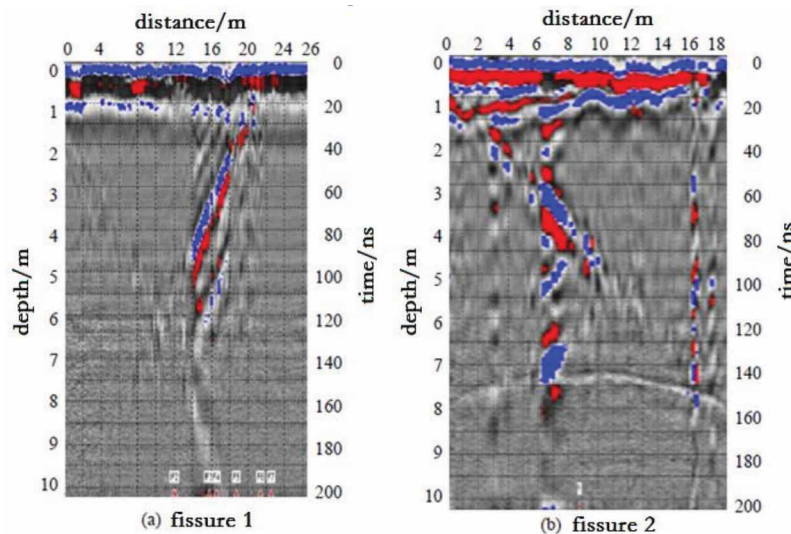


Figure 5—Depths of the fissures extracted from GPR

Field monitoring

To observe the dynamic movement of the surface and the development of ground fissures induced by underground mining, we installed observation stations on the surface above each of these panels. At each panel, we established one line along the mining direction and one line perpendicular to it. All the monitoring points and ground fissures were observed about every four days. On each monitoring day, both the surface movement and the plane positions of ground fissures were measured using a GPS system, and the width and height of the ground fissures were measured using a small steel ruler. The depths of ground fissures were detected using ground penetrating radar (GPR), as shown in Figure 4.

The newly-developed fissures were labelled at the monitoring positions so that observations could be repeated. Each fissure was monitored until it closed completely or stabilized. When the width of the fissure was less than 1 mm, the fissure was considered closed. The time from initial development until complete closure was recorded as the development cycle. To ensure the accuracy of observations, we followed the standards outlined in the Specifications for Global Positioning System (GPS) Surveys (GB/T 18314-2009) and the Specification for GPS Real Time Kinematic (RTK) Measurements (CH/T 2009-2010). We obtained the fissure positions using the real-time kinematic (RTK) function of the GPS system with a precision of 10 mm/km. The width and height difference of the fissure at its centre were measured directly to a precision of 1 mm, and the depth was detected to a precision of 0.1 m, as shown in Figure 5.

Results and discussion

Dynamic features of surface movement and ground fissures

The curve showing changes in the surface subsidence over time, developed from the monitoring results, is shown in Figure 6. The distribution of the measured ground fissures on the three panels is shown in Figure 7, and the development of two fissures is shown in Figure 8.

From the monitoring results, we were able to identify surface movement and the development of the mining-induced ground fissures.

- It can be seen from the surface subsidence curve that

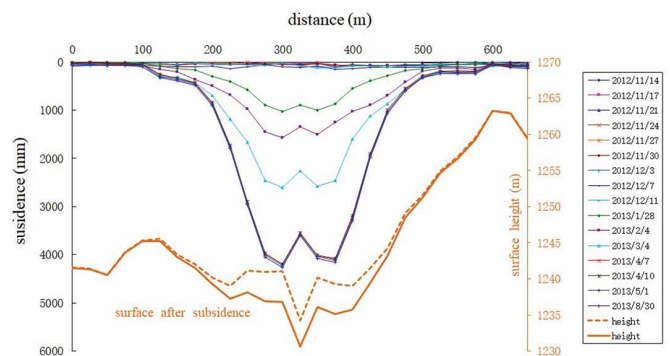


Figure 6—Surface subsidence curve in the direction perpendicular to the advance of panel 52304

Factors that trigger the development of mining-induced ground fissures

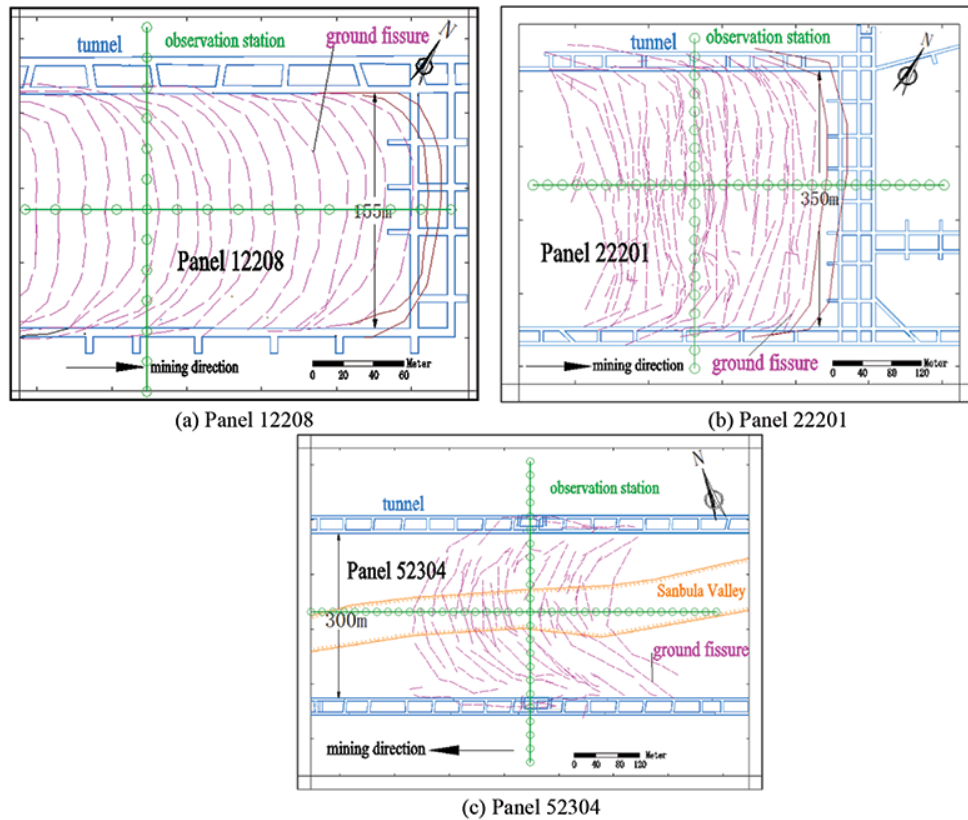


Figure 7—Schematic diagrams of ground fissures and section of the respective panels during mining. Pink dotted lines represent dynamic ground fissures measured during mining, and brown solid lines indicate permanent ground fissures after mining

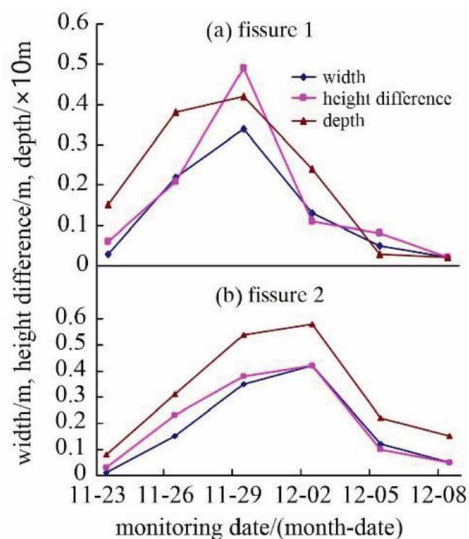


Figure 8—Changes in ground fissure width, height difference, and depth as a function of time

the panel had been fully developed. However, because there was a valley (the Sanbula Valley) on the surface in the centre the panel, while mining caused the overall subsidence of the surface, the soil on both sides slid towards the centre of the valley, and the subsidence of the concave landform decreased. Therefore, the subsidence curve of the central position exhibits a small peak. When the land subsidence ceased, the subsidence in the centre

of the valley was 578 mm less than that of the flat terrain, and the slope of the valley decreased from 15.2 to 13.8 degrees, as shown in Figure 6.

- The high-intensity mining triggered depressions in the ground, and also led to the development of numerous ground fissures at the same time. The fissures were distributed in a C-shape on the whole (Figure 7), similar to the periodic elliptical-shaped fracture that formed in the basic roof of rock strata (Chen *et al.*, 2017; Sun, Yang, and Zhao, 2017), as shown in Figure 9. In the course of the coal face advancing, many dynamic fissures were formed on the surface, which healed gradually, as shown by the pink dotted lines in Figure 7. After mining, ground fissures at the boundary of the panel developed into permanent cracks and were distributed parallel to the mining boundary, and eventually appeared as a C-shape on the ground, as shown in the solid brown lines of Figures 7a and 7b.
- Dynamically, the ground fissures evolved as mining advanced, ahead of the panel face. They first appeared on the surface above the centre of the panel, perpendicular to the direction of advance, and then extended to the goaf boundary. The fissures were widest and deepest in the centre, and gradually became narrower and shallower as they approached the boundary. After mining, the fissures gradually closed, as shown in Figure 8.

Factors that trigger the development of ground fissures

To demonstrate further how the ground fissures developed, we introduced two basic concepts:

Factors that trigger the development of mining-induced ground fissures

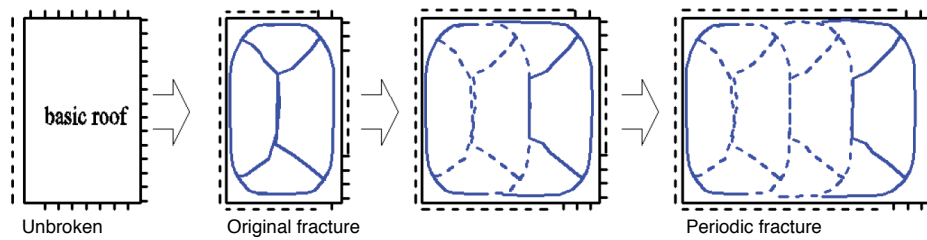


Figure 9—The elliptical-shaped fracture of the basic roof during mining

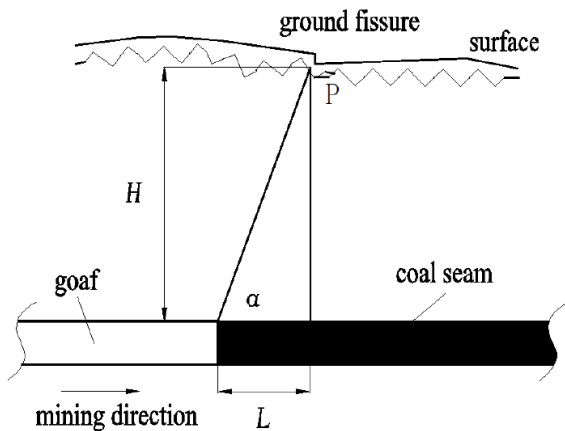


Figure 10—Profile of ground fissure and the panel

- The horizontal distance, L , from a ground fissure to the goaf boundary in the horizontal direction. This is positive when the fissure is ahead of the advance position and negative when behind
- The angle, α , between the line that links the fissure to the goaf boundary and the horizontal line, as shown in Figure 10.

The relationship between L and α is:

$$\tan \alpha = H/L \quad [1]$$

where α = angle of ground fissure (degree)

H = mining depth (m)

L = horizontal distance of ground fissure (m).

We monitored 34 large ground fissures and more than 50 associated small fissures at the site. Summary statistics for the 34 large fissures are listed in Table II. Of these, the horizontal distance was measured *in situ*, the corresponding angle was calculated with Equation [1], and the advance rate was derived from the statistics of the daily mining progress.

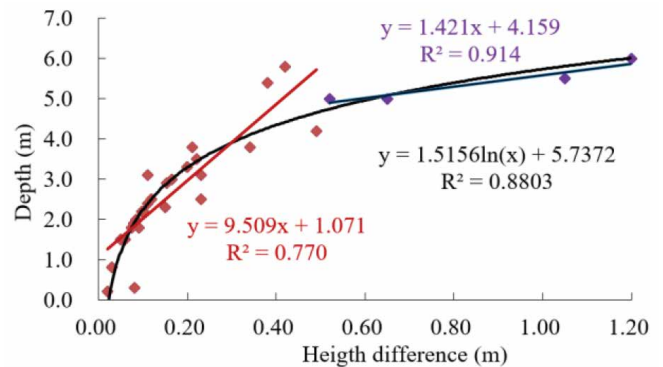


Figure 12—Relationship between depth and height difference of ground fissures

Development law of mining-induced ground fissures

To study how the fissures developed, we used regression analysis to determine the relationship between the width, height difference, and the depth, as shown in Figures 11, 12 and 13, respectively.

$$d = 11.380W + 0.916 \quad [2]$$

$$d = 1.5156 \ln(h) + 5.7372 \quad [3]$$

$$h = 0.0426e^{7.64W} \quad [4]$$

where d = depth of ground fissure (m)

W = width of ground fissure (m)

h = height difference of ground fissure (m).

Figures 11–13 describe the development law of mining-induced ground fissures, as follows.

- There was a significant linear increasing relationship between the depth and the width. In other words, as the width of the surface crack increased, the fissure became deeper, which is consistent with the general development of ground fissures. When there were slight cracks on the surface (cracks that were 0.02 m wide), the fissure began

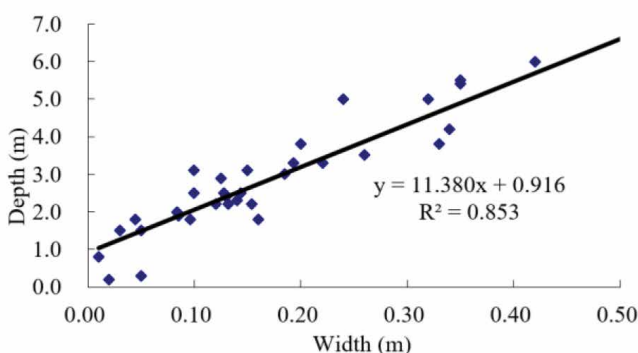


Figure 11—Relationship between depth and width of ground fissures

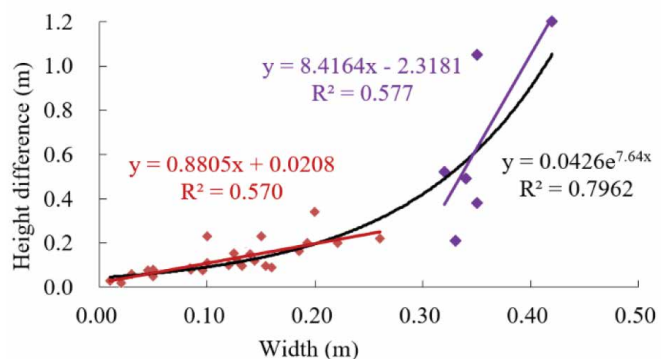


Figure 13—Relationship between height difference and width of ground fissures

Factors that trigger the development of mining-induced ground fissures

Table II

Summary statistics for ground fissures

Case	Width (m)	Height difference (m)	Depth (m)	Horizontal distance (m)	Angle (°)	Surface horizontal deformation (mm/m)	Advance rate (m/d)	Panel
1	0.02	0.02	0.20	23.17	60.17	0.16	2	12208
2	0.01	0.03	0.80	7.50	79.48	0.18	12	
3	0.05	0.05	1.50	28.80	54.52	0.19	1	
4	0.03	0.06	1.50	11.61	73.97	0.21	7	
5	0.05	0.08	0.30	13.22	71.88	0.09	9	
6	0.12	0.10	2.20	17.81	66.21	0.42	3	
7	0.13	0.11	2.40	20.36	63.25	0.59	2	
8	0.33	0.21	3.80	19.95	63.72	0.90	2	
9	0.15	0.23	3.10	17.81	66.21	0.55	5	
10	0.10	0.23	2.50	12.97	72.2	0.33	9	
11	0.20	0.34	3.80	16.31	68.02	0.82	7	
1	0.35	0.38	5.40	4.79	86.22	1.52	12	22201
2	0.51	0.42	5.80	6.90	84.56	1.91	8	
3	0.34	0.49	4.20	9.78	82.32	1.32	2	
4	0.32	0.52	5.00	7.31	84.24	1.36	8	
5	0.24	0.65	5.00	5.43	85.72	1.03	10	
6	0.35	1.05	5.50	6.08	85.21	1.59	11	
7	0.42	1.20	6.00	5.30	85.82	2.13	10	
8	0.19	0.20	3.30	4.32	86.59	0.85	13	
9	0.14	0.12	2.50	3.93	86.9	0.58	13	
10	0.09	0.08	1.90	7.26	84.28	0.39	7	
11	0.19	0.16	3.00	6.23	85.09	0.67	5	
12	0.13	0.10	2.20	9.26	82.72	0.43	3	
1	0.08	0.08	2.00	3.24	87.44	0.31	5	52304
2	0.22	0.20	3.30	1.88	88.51	0.80	10	
3	0.10	0.07	1.80	3.12	87.54	0.41	8	
4	0.15	0.10	2.20	4.16	86.72	0.40	3	
5	0.13	0.15	2.90	4.31	86.6	0.25	3	
6	0.13	0.12	2.50	2.26	88.21	0.41	9	
7	0.05	0.07	1.80	3.12	87.54	0.24	8	
8	0.26	0.22	3.51	3.24	87.44	0.80	5	
9	0.16	0.09	1.80	2.12	88.33	0.41	10	
10	0.14	0.15	2.30	3.12	87.54	0.46	8	
11	0.10	0.11	3.10	3.24	87.44	0.16	6	

to expand longitudinally, and the expansion depth was 0.80 m. The width reached a maximum of 0.51 m during the monitoring, and the fissure extended to a depth of 5.80 m. The correlation coefficient was 0.853. The results from the regression were better, and the coefficient of proportionality of the regression equation was 11.380, which means that, when the width increased by 1 mm, the depth increased by about 114 mm, as shown in Figure 11.

- There was a logarithmic increasing relationship between the depth and height difference, with a correlation coefficient of 0.880. When the height difference increased from zero to 0.5 m, the rate at which the depth increased averaged 9.509, while when the height difference increased by 0.1 m, the depth increased by 0.951 m. When the height difference was greater than 0.5 m, the rate of increase decreased to 1.421; that is, when the height difference increased by 0.1 m, the

depth increased by 0.142 m, and gradually stabilized, as shown in Figure 12.

- There was an exponential increasing relationship between the height difference and width, with a correlation coefficient of 0.5772. When the width increased from zero to 0.26 m, the rate at which the height difference increased averaged 0.8805, while when the width increased by 0.1 m, the height difference increased by 0.088 m. When the width was greater than 0.26 m, the rate of increase increased to 8.4164; that is, when the width increased by 0.1 m, the height difference increased by 0.842 m, and gradually stabilized, as shown in Figure 13.

Relationship between fissure width and surface horizontal deformation

We used regression analysis to determine the relationship

Factors that trigger the development of mining-induced ground fissures

between the fissure width and the surface horizontal deformation, as shown in Figure 14.

$$W = 0.221\varepsilon + 0.027 \quad [5]$$

where ε = surface horizontal deformation (mm/m).

When the surface horizontal deformation reached 0.16 mm/m, fissures began to develop, and the width was 0.02 m. The maximum width during the monitoring was 0.51 m, at which point the horizontal deformation was 1.91 mm/m. There was an obvious linear increasing relationship between the fissure width and the horizontal deformation at the surface. As the deformation increased, the width of the fissure also increased, and the width increased by 0.221 m when the horizontal deformation increased by 1 mm/m, as shown in Figure 14.

Relationship between ground fissure development and advance rate

In conventional mining conditions, a ratio of mining depth to extraction height of 30 is often considered the critical value for discontinuous surface deformation. However, for shallow coal seams, the tensile strength of the soil in the unconsolidated layer is weak and is often negligible. Therefore, when the rock strata fracture, the ground will suffer from discontinuous deformation, and the thickness of the rock strata may be a more useful metric than the mining depth. Many studies have found that more ground fissures developed as the ratio of the rock strata thickness to the extraction height increased. Meanwhile,

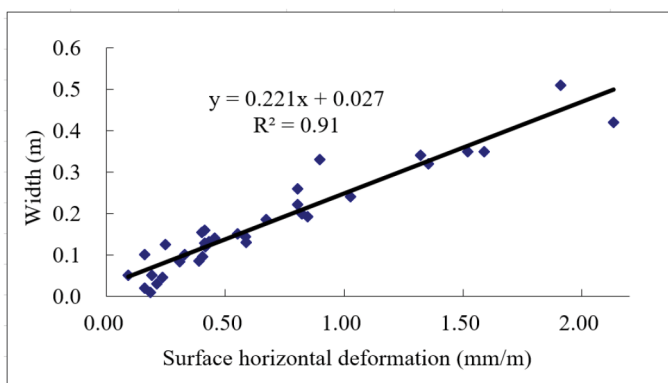


Figure 14—Relationship between width of the ground fissure and surface horizontal deformation

as the advance rate of the panel decreased, the number of ground fissures increased. Therefore, the geological parameters, namely the thickness of rock strata and the extraction height of the coal seam, and the advance rate of panel are considered the main influences on the development of mining-induced ground fissures. We defined a variable called the comprehensive impact parameter, which is the product of the advance rate and the ratio of the rock strata thickness to the extraction height.

$$K = v * h/m \quad [6]$$

where K = comprehensive impact parameter (m/d)

v = advance rate of panel (m/d)

h = thickness of rock strata (m)

m = extraction height of coal seam (m).

The relationships between the comprehensive impact parameter and the horizontal distance or angle of ground fissure can be expressed by the following equations and are shown in Figure 14:

$$L = -5.7324 \ln(K) + 33.483 \quad [7]$$

$$\alpha = 8.0032 \ln(K) + 45.590 \quad [8]$$

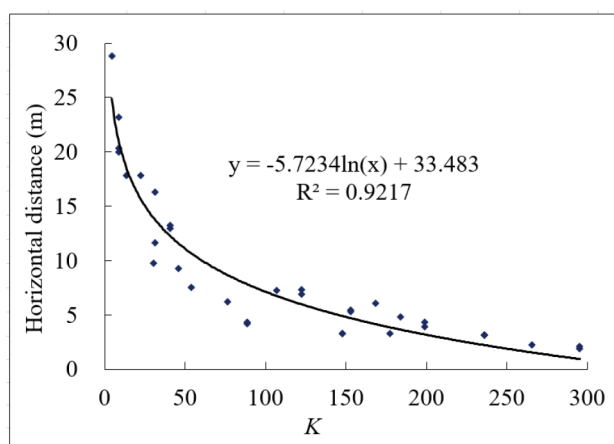
There was a significant negative logarithmic relationship between the horizontal distance and K , and a significant positive logarithmic relationship between the angle and K , with correlation coefficients of 0.9217 and 0.8947, respectively. The regression effect was therefore very good.

As the K value increased, the horizontal distance increased and the angle decreased, both logarithmically. When K increased from zero to 150, the horizontal distance decreased rapidly from about 30 m to 5 m, while the angle increased rapidly from 55° to 85°. When K increased from 150 to 300, the horizontal distance decreased slowly, and eventually approached zero, while the angle increased slowly and eventually approached 90°. In other words, when K was greater than 150, the development of the ground fissures was almost synchronous with the coal seam excavation.

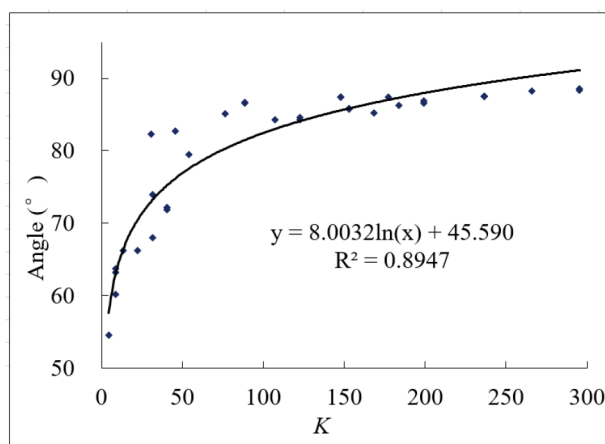
Technology for mitigating mining-induced ground fissures

Standards for mitigating dynamic ground fissures

Because dynamic fissures self-heal during the mining process, scholars have proposed that dynamic fissures generally do not need to be mitigated until the ground has subsided and is stable.



(a) L vs. K



(b) α vs. K

Figure 14—The relationships between the comprehensive parameter K and (a) the horizontal distance L and (b) angle α of the ground fissure

Factors that trigger the development of mining-induced ground fissures

In normal conditions, the overlying rock strata are generally disrupted and surface movement occurs during underground mining. The damage includes three zones, namely the caved zone, the fractured zone, and the continuous bending zone from the roof of rock strata to the surface. The caved zone and the fractured zone are also called the water-flowing fractured zone. However, in mining areas with large extraction heights, shallow depths, and thick unconsolidated layers, a large number of ground fissures often develop. Once the upward-moving fractured zone of rock strata comes into contact with the downward-extending ground fissures, the safety of underground mining will be compromised, and there may be outbursts of water and sand, and gas leakages. In particular, the fractured zone frequently reaches the surface when the rock strata are thick, and the ground fissures become collapsing cracks, and the hidden dangers are even more pronounced.

Thus, given the risks to safety of underground mining, based on the relationship between the width or height difference and the depth of ground fissures, and considering the empirical formula of the water-flowing fractured zone, we propose a standard for managing dynamic ground fissures. That is, when the sum of the water-flowing fractured zone height and the ground fissure depth is greater than the mining depth, dynamic fissures should be managed. This can be expressed as follows:

$$d + H_w \geq H \quad [9]$$

where H_w = height of the fractured zone (m)

H = mining depth (m).

Furthermore, $d_{max} = H - H_w$ may be defined as the maximum safe depth of dynamic fissures, and Equations [2] and [3] can be substituted into the expression. The maximum safe width or the maximum height difference of a dynamic ground fissure can therefore be expressed as follows:

$$W_{max} = \frac{H - H_w - 0.916}{11.380} \quad [10]$$

$$h_{max} = e^{\frac{H - H_w - 5.7372}{1.5156}} \quad [11]$$

where W_{max} = maximum safe width (m)

h_{max} = maximum safe height difference (m).

It is difficult to detect the depth of a ground fissure, but it is easier to measure the width and height difference. We therefore propose that the maximum safe width or the maximum safe height difference are considered as the standards for managing dynamic fissures. That is, when the width of a dynamic fissure is greater than the value in Equation [10], or the height difference is greater than the value in Equation [11], this means that the ground fissure has connected with the water-flowing fractured zone of rock strata. As a result, to ensure that the mining

operations can continue safely, the dynamic ground fissures need to be mitigated.

Engineering practice

To mitigate dynamic ground fissures that develop during underground mining, the following approach can be adopted.

First, a system should be set up to evaluate ground fissure disasters. Then the height of the water-flowing fractured zone of rock strata and the depth of the ground fissure should be predicted from the geological and mining conditions of the panel, and a grading system established with which to robustly evaluate how the ground fissure might impact on the safety of underground mining. The maximum safe width or height difference of ground fissures at which production safety is affected should be determined. A monitoring network should then be set up to monitor the fissures in real time, and the monitoring period should be determined from the advance rate. The dynamic fissures can then be managed. Dynamic fissures are treated differently from permanent fissures, and the main aim of the treatment is to prevent the underground stope connecting the surface, so that surface wind-blown sediment, loess, or accumulated water cannot enter the panel, and underground ventilation is maintained. Therefore, measures to treat dynamic ground fissures should be taken, such as filling fissures, and levelling the surface.

In Daliuta coal mine, panels 12208, 22201, and 52304 were, on average, 40.4, 73.0, and 234.9 m deep respectively, and the heights of the fractured zone of rock strata were 64.2, 49.7, and 62.7 m, respectively. In panel 12208, the fractured zone reached the surface, therefore all dynamic fissures needed to be treated. In panel 22201, the maximum safe width of the ground fissure was 1.88 m, calculated from Equation [10]. Field monitoring showed that the maximum width of the ground fissure was 0.44 m, and because it had not reached the control standard, the fissure did not need to be mitigated. The maximum safe width of the ground fissure in panel 52304 was 13.1 m, calculated from Equation [10]. Field monitoring showed that the maximum width of the developed ground fissure was 1.23 m, which was much less than the standard and so it did not need to be mitigated either. The development of dynamic ground fissures at the three panels is shown in Figure 15.

Conclusions

- With the Shendong mining area as the study site, we carried out a field survey to examine how mining-induced ground fissures developed, and found that:
 - (a) The development of dynamic fissures involved three phases, known as 'crack-extension-closure'
 - (b) During coal seam excavation, ground fissures developed ahead of the advance position, and formed a C-shape feature



(a) Panel 12208



(b) Panel 22201



(c) Panel 52304

Figure 15—Dynamic ground fissures above the three panels

Factors that trigger the development of mining-induced ground fissures

(c) Ground fissures were distributed in an elliptical shape on the boundary of the panel when the ground stabilized after subsidence.

- ▶ We studied the main influences on mining-induced ground fissures and established relevant empirical models. The relationship between the fissure width and the surface deformation, and a model to predict the fissure depth, were established. We propose the comprehensive impact parameter K so that a dynamic prediction model of the angle and the horizontal distance of ground fissures could be established.
- ▶ We propose a standard for managing dynamic ground fissures that is based on the empirical formula for the height of the water-flowing fractured zone and the model for predicting the depth of the ground fissure. The standard is the maximum safe width or the maximum safe height difference. We tested this standard on three panels with different mining depths in the Daliuta coal mine.
- ▶ In this study, we focused on the geological mining conditions of coal seams with thick unconsolidated layers, thin rock strata, and shallow mining depth in western China. Our methods for managing ground fissures need to be verified further in real-life situations. As mining-induced ground fissure disasters are influenced by various factors, such as the geological and mining environment, topographic conditions, and physical and mechanical properties of the rock and soil, the conditions and development rules are more complex than those discussed here. We hope that additional studies and research results will be published in the near future.

Acknowledgements

This study was supported by Chinese Major Project of National Social Science Foundation (No.14ZDB145), and the Research Fund of The State Key Laboratory of Coal Resources and safe Mining, CUMT (No. SKLCRSM 15KF06), and the Key Project of Natural Science Research in Anhui Colleges and Universities, China (No. KJ2018A0002).

References

- BIAN, Z.F., MIAO, X.X., LEI, S.G., CHEN, S.E., WANG, W.F., and STRUTHERS, S. 2012. The challenges of reusing mining and mineral-processing wastes. *Science*, vol. 337, no. 6095. pp. 702–703.
- CHEN, D.D., HE, F.L., XIE, S., GAO, M.M., and SONG, H.Z. 2017. First fracture of the thin plate of main roof with three sides elastic foundation boundary and one side coal pillar. *Journal of China Coal Society*, vol. 42, no. 10. pp. 2528–2536.
- DAGVADORJ, L., BYAMBA, B., and ISHIKAWA, M. 2018. Effect of local community's environmental perception on trust in a mining company: A case study in Mongolia. *Sustainability*, vol. 10, no. 3. pp. 614–626.
- FINFINGER, G. and PENG, S. 2016. Guest editorial: Special issue on Ground Control in Mining in 2016. *International Journal of Mining Science and Technology*, vol. 26, no. 1. pp. 1–2.
- GAUR, V.P., KAR, S.K., and SRIVASTAVA, M. 2015. Development of ground fissures: A case study from southern parts of Uttar Pradesh, India. *Journal of the Geological Society of India*, vol. 86, no. 6. pp. 671–678.
- GHABRAIE, B., REN, G., and SMITH, J.V. 2017. Characterising the multi-seam subsidence due to varying mining configuration, insights from physical modelling. *International Journal of Rock Mechanics and Mining Sciences*, vol. 93. pp. 269–279.
- HAN, K.F., KANG, J.R., WANG, Z.S., and WU, K. 2014. Prediction of surface fissure in high relief areas induced by underground coal mining. *Journal of Mining and Safety Engineering*, vol. 31, no. 6. pp. 896–900 [in Chinese].
- HARTLIEB, P., GRAFE, B., SHEPEL, T., MALOVYK, A., and AKBARI, B. 2017. Experimental study on artificially induced crack patterns and their consequences on mechanical excavation processes. *International Journal of Rock Mechanics and Mining Sciences*, vol. 100. pp. 160–169.
- HE, Y.M., HE, X., LIU, Z.R., ZHAO, S.W., BAO, L.Y., LI, Q., and YAN, L. 2017. Coal mine subsidence has limited impact on plant assemblages in an arid and semi-arid region of northwestern China. *Ecoscience*, vol. 24. pp. 91–103.
- HU, Z.Q., WANG, X.J., and HE, A.M. 2014. Distribution characteristic and development rules of ground fissures due to coal mining in windy and sandy region. *Journal of China Coal Society*, vol. 39, no. 1. pp. 11–18 [in Chinese].
- ISHWAR, S.G. and KUMAR, D. 2017. Application of DInSAR in mine surface subsidence monitoring and prediction. *Current Science*, vol. 112, no. 1. pp. 46–51.
- LI, H.X., LEI, S.G., and SHEN, Y.Q. 2016. Impacts of ground subsidence and fissures caused by coal mining on vegetation coverage. *Journal of Ecology and Rural Environment*, vol. 32, no. 2. pp. 195–199.
- LIU, H., DENG, K.Z., LEI, S.G., and BIAN, Z.F. 2015. Mechanism of formation of sliding ground fissure in loess hilly areas caused by underground mining. *International Journal of Mining Science and Technology*, vol. 25, no. 4. pp. 553–558.
- LIU, H., HE, C.G., DENG, K.Z., BIAN, Z.F., FAN, H.D., LEI, S.G., and ZHANG, A.B. 2013. An analysis of forming mechanism of collapsing ground fissure caused by mining. *Journal of Mining and Safety Engineering*, vol. 30, no. 3. pp. 380–384 [in Chinese].
- MALINOWSKA, A.A. and HEJMANOWSKI, R. 2016. The impact of deep underground coal mining on earth fissure occurrence. *Acta Geodynamica et Geomaterialia*, vol. 13, no. 4. pp. 321–330.
- MOHSENI, N., SEPEHR, A., HOSSEINZADEH, S.R., GOLZARIAN, M.R., and SHABANI, F. 2017. Variations in spatial patterns of soil-vegetation properties over subsidence-related ground fissures at an arid ecotone in northeastern Iran. *Environmental Earth Sciences*, vol. 76, no. 6. pp. 2334–2346. <https://www.springerprofessional.de/en/variations-in-spatial-patterns-of-soil-vegetation-properties-ove/12144660>
- PENG, J.B., XU, J.S., MA, R.Y., and WANG, F.Y. 2016. Characteristics and mechanism of the Longyao ground fissure on North China Plain, China. *Engineering Geology*, vol. 214. pp. 136–146.
- SALMI, E.F., NAZEM, M., and KARAKUS, M. 2017a. Numerical analysis of a large landslide induced by coal mining subsidence. *Engineering Geology*, vol. 217. pp. 141–152.
- SALMI, E.F., NAZEM, M., and KARAKUS, M. 2017b. The effect of rock mass gradual deterioration on the mechanism of post-mining subsidence over shallow abandoned coal mines. *International Journal of Rock Mechanics and Mining Sciences*, vol. 91. pp. 59–71.
- SONG, S.J., ZHAO, X.G., ZHANG, Y., and NIE, W.J. 2016. Analyzing the effect of the mining depth on the shape and erosion of surface slope in coal mining area. *Environmental Science and Technology*, vol. 39, no. 8. pp. 178–184.
- SUN, J., YANG, H., and ZHAO, G. 2017. Relationship between water inrush from coal seam floors and main roof weighting. *International Journal of Mining Science and Technology*, vol. 27, no. 5. pp. 873–881.
- SUN, Y.H., ZHANG, X.D., MAO, W.F., and XU, L.N. 2015. Mechanism and stability evaluation of goaf ground subsidence in the third mining area in Gong Changling Area, China. *Arabian Journal of Geosciences*, vol. 8, no. 2. pp. 639–646.
- TOST, M., HITCH, M., CHANDERKAR, V., MOSER, P., and FEIEL, S. 2018. The state of environmental sustainability considerations in mining. *Journal of Cleaner Production*, vol. 182. pp. 967–977.
- WANG, S.F., LI, X.B., and WANG, S.Y. 2017. Separation and fracturing in overlying strata disturbed by longwall mining in a mineral deposit seam. *Engineering Geology*, vol. 226. pp. 257–266.
- YANG, J.H., YU, X., YANG, Y., and YANG, Z.Q. 2018. Physical simulation and theoretical evolution for ground fissures triggered by underground coal mining. *Plos One*, vol. 13, no. 3. pp. e0192886.
- YANG, M., MEN, Y.M., YUAN, L.Q., and YANG, L.W. 2016. Numerical analysis of subway vibration responses for different tunnel types in ground fissure areas. *Journal of Disaster Prevention and Mitigation Engineering*, vol. 36, no. 2. pp. 188–195.
- YIN, Z.Y. and DONG, H. 2015. Impact parameters of SHM for thick coal seam mining of open-pit slope based on slope stability. *Journal of Basic Science and Engineering*, vol. 23, no. 1. pp. 56–67.
- ZHANG, A., LU, J., and KIM, J.W. 2018. Detecting mining-induced ground deformation and associated hazards using spaceborne InSAR techniques. *Geomatics Natural Hazards and Risk*, vol. 9, no. 1. pp. 211–223.
- ZHAO, C.Y., ZHANG, Q., DING, X.L., LU, Z., YANG, C.S., and QI, X.M. 2019. Monitoring of land subsidence and ground fissures in Xian, China 2005–2006: Mapped by SAR interferometry. *Environmental Geology*, vol. 58, no. 7. pp. 1533–1540 [in Chinese].
- ZHAO, K.Y., XU, N.X., MEI, G., and TIAN, H. 2016. Predicting the distribution of ground fissures and water-conducted fissures induced by coal mining: a case study. *Springerplus*, vol. 5, no. 1. pp. 1–23.
- ZHU, X.J., GUO, G.L., LIU, H., CHEN, T., and YANG, X.Y. 2019. Experimental research on strata movement characteristics of backfill-strip mining using similar material modeling. *Bulletin of Engineering Geology and the Environment*. vol. 78. pp. 2151–2167. ◆